Biol. Stud. 2020: 14(3); 3–12 • DOI: https://doi.org/10.30970/sbi.1403.625
www.http://publications.lnu.edu.ua/journals/index.php/biology

UDC: 577.3+612.15+616.006.3

# DYNAMIC CONTRAST ENHANCED $^{1}$H-MAGNETIC RESONANCE IMAGING IN ASSESSMENT OF SKELETAL MUSCLE AND FIBROSARCOMA PERFUSION

***A. Babsky*** [1]***, N. Bansal*** [2]

[1] *Ivan Franko National University of Lviv, 4, Hrushevskyi St., Lviv 79005, Ukraine*

[2] *Department of Radiology and Imaging Sciences, Indiana University, Indianapolis, IN 46202, USA*

**Corresponding author: e-mail: andriy.babsky@lnu.edu.ua*

*Babsky A., Bansal N.* Dynamic contrast enhanced $^{1}$H-magnetic resonance imaging in assessment of skeletal muscle and fibrosarcoma perfusion. **Studia Biologica**, 2020: 14(3); 3–12 • DOI: https://doi.org/10.30970/sbi.1403.625

**Background.** The detection of neoplastic transformation and prediction of the therapeutic response are very important for effective cancer therapy. Current assessment of tumor treatment efficacy relies on evaluating changes in the tumor size or volume, weeks to months after the assumption of a therapeutic protocol. The tissue perfusion is one of the most important parameter to estimate the neoplastic progress and the efficacy of antitumor therapy. $^{1}$H-magnetic resonance imaging (MRI) is an effective tool that provides distinctive information related to structural, cellular, apoptotic, and necrotic changes in tumor tissue. The technique can be used widely for tumor detection and monitoring of the response to treatment.

**Methods.** Dynamic contrast enhanced $^{1}$H-MRI was used for the assessment of tumor perfusion parameters in normal muscle and in subcutaneous Radiation Infused Fibrosarcoma – 1 (RIF-1) developed under the skin in C3H mice. Gadolinium (20 mM) was used as a capillaries perfusion tracer. Therapy of RIF-1 was administered by a single intraperitoneal injection of 5-fluorouracil (150 mg/kg). MRI experiments were performed before and 3 days after the treatment.

**Results.** Dynamic contrast enhanced $^{1}$H-MRI has shown a much lower perfusion rate in RIF-1 tumor compared to skeletal muscle. 5-fluorouracil caused a significant decrease in subcutaneous RIF-1 volume on days 2 and 3 post-treatment, as well as an increase in tumor inflow measured by Dynamic contrast enhanced $^{1}$H-MRI. An increase in tumor tissue perfusion correlated with an increase in tissue apparent diffusion coefficient and total $Na^{+}$ concentration following 5-fluorouracil chemotherapy reflect an increase in extracellular space and vasodilatation. On the other hand, as it was shown in our previous publications, the lower intracellular $Na^{+}$ concentration and glucose uptake

in treated by 5-fluorouracil tumors compared with control tumors suggest a shift in tumor metabolism from glycolysis to oxidation and/or a decrease in cell density.

**Conclusions.** Method of dynamic contrast enhanced $^{1}$H-MRI in combination with other NMR methods, positron emission tomography, histology, etc. should prove useful in assessment of neoplastic transformation of tumor capillaries and efficacy of chemotherapy.

***Keywords:*** muscle, perfusion, Gadolinium, fibrosarcoma, 5-fluorouracil, $^{1}$H-MRI

## INTRODUCTION

Biological tissues hemodynamics plays an important role in normal and tumor tissues including an incretion and excretion of antitumor drugs. Several methods have been proposed for the quantification of tumor perfusion, such as a clearance of xenobiotics, single-photon emission computerized tomography, positron emission tomography, and diffusion weighted $^{1}$H-MRI (DWI) [23]. Dynamic contrast enhanced (DCE) $^{1}$H-magnetic resonance imaging (MRI) reflects perfusion in microvessels. This method has a good potential value in characterizing muscle pathological changes, differentiating between malignant and benign sarcomas, monitoring response to chemotherapy [20, 22, 24] and predicting clinical efficacy of vascular disrupting agents with good imaging-histopathology correlation [12].

5-Fluorouracil (5FU) belongs to the antimetabolite and pyrimidine analog family of antitumor medication [21]. It is involved in blocking the action of thymidylate synthase and thus stopping the production of DNA [1]. It was shown that RIF-1 tumor volumes decreased in 5FU-treated mice [4]. $^{23}$Na and $^{1}$H MRI experiments show that this 5FU effect was correlated with an increase in both total tissue $Na^{+}$ level and water apparent diffusion coefficient (ADC) whereas intracellular $Na^{+}$ level and glucose uptake in treated tumors were lower compared with control tumors [2]. We hypothesized that a shift of energetic metabolism to oxidative phosphorylation has to be related to a better supply of oxygen to the treated tumor tissue. However, the possible role of tissue perfusion in 5FU antitumor effects was not clarified yet.

The goal of this paper was to estimate the possibility of applying DCE method in monitoring of blood perfusion in normal muscle tissue and radiation infused fibrosarcoma (RIF-1) treated with effective chemotherapeutic agent.

## MATERIALS AND METHODS

**RIF-1 Tumor Model**. All animal studies were approved by the Indiana University Institutional Animal Care and Use Committee. RIF-1 tumor cells were grown in monolayers using minimum essential medium (MEM; Mediatech, Herdon, VA, USA) supplemented with 10% fetal bovine serum, 10 mM HEPES, and 1% penicillin under a 5% $CO_2$ and 95% $O_2$ atmosphere at 37 °C. The tumor cells were passaged between *in vitro* and *in vivo* states according to the protocol [2].

Male C3H/HeN mice (Harlan, Indianapolis, IN, USA), approximately 6 weeks old and weighing 18 to 20 g, were inoculated in the right or left thigh (region of *m. biceps femoris* and *m. gluteus maximus*) with a subcutaneous (sc) injection of $\sim 2\times10^{6}$ cells in 0.10 to 0.15 mL volume of Hank's balanced salt solution. Animals were anesthetized with an intraperitoneal (ip) injection of 50 mg/kg ketamine, 5 mg/kg acepromazine, and 0.25 mg/kg atropine. The tumors were allowed to grow for 2 to 3 weeks to a volume of 0.7 to 1.0 $cm^3$ before performing the first MRI experiment. Tumor growth was monitored

by caliper measurement. Tumor volume was calculated from three orthogonal diameters (x, y, and z) using the formula (π/6)xyz. Ten tumor-bearing mice were treated with a single dose of 5FU (150 mg/kg, ip; Sigma-Aldrich, St. Louis, MO, USA) for tumor volume estimation. Nine animals served as untreated controls.

***In Vivo* MRI Experiments**. All *in vivo* MRI experiments were performed on a 9.4-T, 31-cm horizontal bore system (Varian, Palo Alto, CA, USA) equipped with a 12-cm-diameter shielded gradient set capable of up to 40 G/cm in three directions. A loop-gap resonator (inner diameter = 30 mm, depth = 25 mm) tuned to 400 MHz for $^1$H was used to collect DCE $^1$H-MRI of the muscle and tumor. The animals were anesthetized with 1–1.5% isoflurane delivered in medical air at 1.0–1.5 L/min using a mouse nose mask connected to a gas anesthesia machine (Vetland, Louisville, KY, USA). Animals were positioned on top of a custom-designed plastic cradle with the tuned loop-gap resonator attached to it [2]. The right or left thigh with subcutaneous tumor was positioned inside the resonator, and the animal was held in place with a tape. A detachable cylindrical phantom (6.5 mm diameter and 23 mm length) consisting of distillate water was also placed inside the resonator to serve as a water MRI standard. Warm air was blown through the magnet bore to maintain the rectal animal temperature during the MRI experiments (1–1.5 h) at 32–36 °C. The temperature was monitored with a fiber optic probe (FISO Technologies, Inc., Quebec, Canada). The magnet was shimmed to less than 100 Hz line width at half height of the $^1$H water signal. The MRI experiments were performed prior to treatment with 5FU (150 mg/kg) and on day 3 after treatment.

**DWI.** Multi-slice DWI was collected using a modified spin-echo sequence and the following parameters: repetition time (TR) = 1000 ms, echo time (TE) = 1000 ms/21 ms, $\delta$ = 6 ms, $\Delta$ = 11 ms, matrix size = 256×128, field of view (FOV) = 80 mm×80 mm, number of slices = 12, slice thickness = 0.5 mm, slice gap =1.5 mm.

**DCE $^1$H MRI.** After collecting a baseline of DWI, 0.2 mmol/kg of Gadolinium-DOTA was manually injected over a 30 s interval through a 26-gauge catheter placed in the tail vein. Contrast agent Gadolinium-DOTA is commonly used for DCE MRI showing appropriate changes of tissue perfusion without damages of capillaries [16]. All bolus injections were performed by the same investigator. DCE $^1$H-MRI was obtained using a gradient-echo sequence and the following parameters: TR/TE = 10 ms/3.1 ms, matrix size = 256×128, FOV = 64 mm×64 mm, number of slices = 1, and slice thickness = 4 mm. 200 images were collected over approximately 13 min, with 4.5 s acquisition time per image.

**Data analysis.** $^1$H images were reconstructed using the Image Browser software (Varian, Palo Alto, CA, USA). PSI-PLOT software was used to analyze DCE $^1$H-MRI data. The kinetics of contrast agent uptake was estimated by measuring the area under the curve over the first 60 s after the contrast agent arrival, as well as by fitting the DCE $^1$H-MRI signal intensity versus time data to a triexponential function [5].

Tumor volume changes are presented as the mean ± standard error of mean (SEM) and represent the range across a cohort of animals. Statistical analyses of the data were performed by ANOVA (Statistica/v. 5.1 program). $P \leq 0.05$ was used to define statistical significance in tumor volume changes.

All animal studies were approved by the Indiana University Institutional Animal Care and Use Committee.

## RESULTS and DISCUSSION

**Effect of 5FU on Tumor Growth**. The mean tumor volumes of control and treated mice are shown in **Fig 1**. Before treatment, both groups had similar tumor volumes

(0.72 ± 0.03 cm$^3$ for control group, 0.77 ± 0.05 cm$^3$ for treated group). Baseline of tumor volume in both control and 5FU treated groups was taken as 100%. In 5FU-treated animals, the mean tumor volume decreased by 38% (P ≤ 0.05 vs pretreatment) on day 2 and by 54% (P ≤ 0.05 vs pretreatment) on day 3 after treatment. The mean tumor volumes in control animals grew by 14% on day 2 and by 18% on day 3 and were larger (P ≤ 0.05) than the tumor volumes 2 and 3 days after treatment.

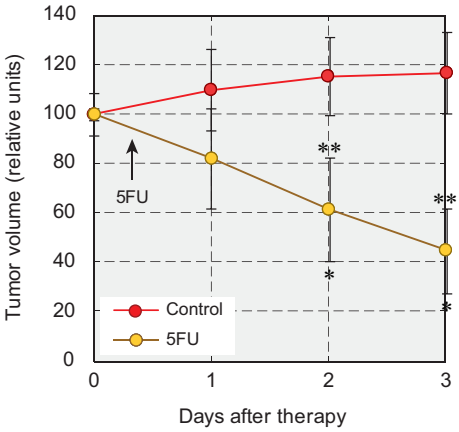


**Fig. 1.** Effect of 5-fluouracil (5FU, 150 mg/kg) on subcutaneous RIF-1 tumor volume. Tumor volume was estimated using $^1$H-MRI (M±m). Baseline of tumor volume before therapy was taken as 100%. Significance: P ≤ 0.05 (* – vs. Day 0; ** – Control vs. 5FU)

**Рис. 1.** Вплив 5-фторурацилу (5ФУ, 150 мг/кг) на об'єм підшкірної радіаційно-індукованої фібросаркоми. Об'єм пухлини обчислювали на підставі зображень $^1$H-МРТ. Об'єм пухлин до терапії приймали за 100%. Достовірність: P ≤ 0.05 (* – vs. День 1; ** – Контроль vs. 5ФУ)

**Fig. 2** shows the representative $^1$H-MRI images before (images 1 and 2) and throughout (images 3–9) accumulation of perfusion tracer Gadolinium by a mouse C3H muscle (marked by dotted red line) and by subcutaneous RIF-1 (dotted yellow line). Gadolinium (20 mM) was delivered to animal through the tail vein. To enhance the difference of MRI signals after Gadolinium treatment the baseline image 2 was extracted from each image 3–9 and marked as images 3′–9′. Delivering of the perfusion tracer to tissue microvessels is accompanied by an increase in brightness of the image. It is visible that DCE in the muscle started much earlier (images 4 and 4′) than in subcutaneous RIF-1 (images 7 and 7′). The difference between DCE in muscle and tumor disappeared in images 9 and 9′ only.

The representative DCE $^1$H-MRI signal intensity vs. time curves in the mouse muscle (*m. biceps femoris* and *m. gluteus maximus*) and subcutaneous RIF-1 are presented in **Fig. 3**. The rate of perfusion was calculated as a slope of the tracer permeability or outflow curves and was calculated as tg of angle $\alpha$. The permeability rate following very next to the Gadoilinium bolus had a biexponential shape. During this period, the rate of perfusion in muscle was much higher compared to tumor: 19.1 and 8.14 (in muscle) and 8.14 and 2.14 (in tumor). After this period, the equilibrium of tracer inflow and outflow was observed, but the duration of this step was much shorter in muscle (130 c) than in tumor (430 c). During 450–1500 s (muscle) and 750–1500 s (tumor) the tracer washout rates were equal (tg $\alpha$ = -2.48) in both tissues.

The DCE $^1$H-MRI in tumor *vs.* muscle ratio are presented in **Fig. 4**. Both traces were monitored on the same mouse before (pink dots) and 3 days after (dark blue dots) treatment with 5FU. Light blue and yellow lines represent linearized data points for before and after treatment cases, respectively. Baselines (before Gadolinium bolus) of DCE in tumor *vs.* muscle ratios were normalized to one. We assumed that DCE in normal muscle is relatively stable in both before and after treatment circumstances. Thus, all differences presented in the **Fig. 4** are caused mainly by DCE changes in the tumor.

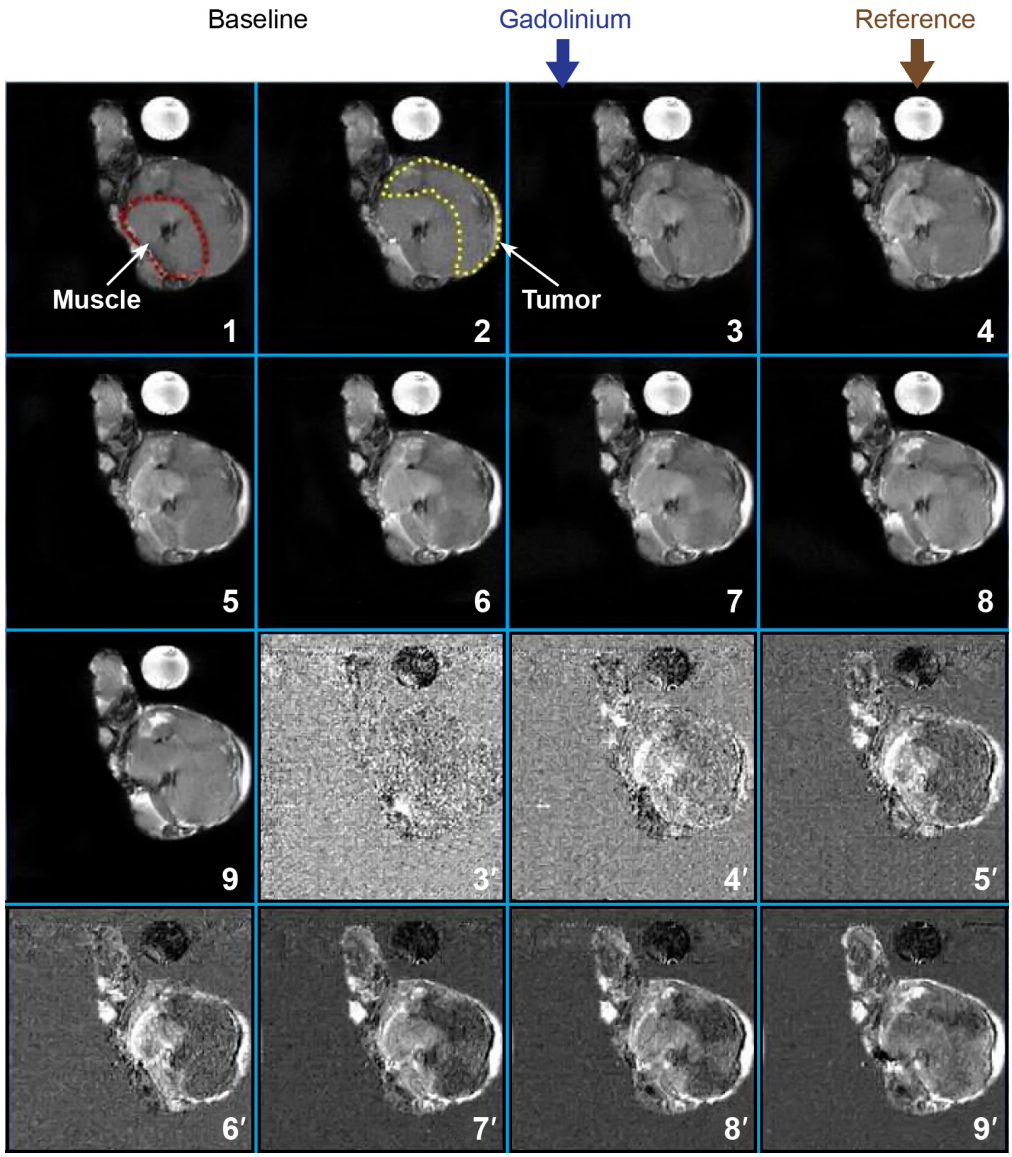


**Fig. 2.** Corresponding Dynamic Contrast Enhanced $^{1}$H MRI images before (images 1 and 2) and throughout (images 3–9) accumulation of perfusion tracer Gadolinium by skeletal muscle (marked by dotted red line) and by subcutaneous RIF-1 (dotted yellow line) developed in a C3H mouse. Gadolinium (20 mM) was delivered through the tail vein. To enhance the difference of MRI signals after the Gadolinium injection the baseline image 2 was extracted from each images 3–9 and marked as images 3′–9′. The reference, distillate water, was placed in plastic tube next to the mouse back thigh

**Рис. 2.** Динамічно-контрастні $^{1}$H-МРТ зображення до (1 і 2) і впродовж (3–9) акумулювання перфузійного маркера ґадолінію скелетними м'язами (помічені червоною переривчастою лінією) і підшкірною радіаційно-індукованою фібросаркомою (жовта переривчаста лінія), прищепленою на задній лапці миші лінії С3Н. Ґадоліній (20 мМ) вводили через хвостову вену. Для покращення візуалізації МРТ-сигналу після введення ґадолінію базове зображення (2) "екстрагували" з кожного із зображень 3–9 і позначали як 3′–9′. Для стандарту використовували дистильовану воду, яку поміщали у пластиковій трубці біля задньої лапки миші

The response to the Gadolinium injection was different before and after treatment. During the first 100–150 s period following the Gadolinium bolus, the inflow of tracer in the untreated tumor decreased by 40% (tg $\alpha$ = -0.18) while after treatment the inflow increased by 20% (tg $\alpha$ = 3.49). During the next 150 s period, which corresponds to the equilibrium period (see Fig. 3), the rate of perfusion in the treated tumor was still higher compared to the untreated tumor. Thus, these data show that after treatment with 5FU the rate of tumor permeability is higher. ~ 300 s after the Gadolinium injection the DCE of tumor to muscle ratio became equal for both cases. During the next period up to 1500 s, representing mostly balance between inflow and washout, the DCE ratio of tumor *vs.* muscle was slightly higher in before treatment (tg $\alpha$ = 0.31) compared to after treatment case (tg $\alpha$ = 0.16).

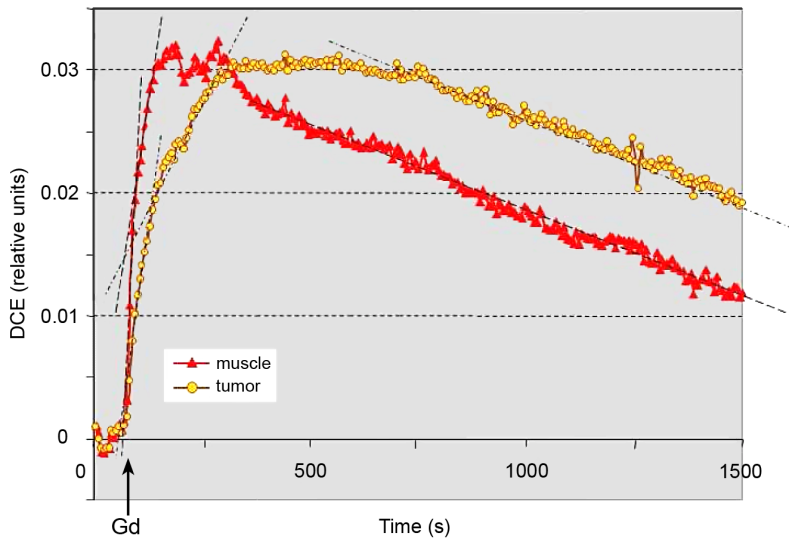


**Fig. 3.** Representative experiment of Diffusion Contrast Enhancement (DCE) $^{1}$H-MRI in muscle and subcutaneous RIF-1 developed in a C3H mouse. Gd – Gadolinium. DCE $^{1}$H-MRI before Gd-bolus (baseline) was taken as 0

**Рис. 3.** Репрезентативний експеримент відносних змін інтенсивності динамічно-контрастних $^{1}$H-МРТ-зображень у скелетних м'язах (muscle) і підшкірній радіаційно-індукованій фібросаркомі (tumor) миші лінії С3Н після ін'єкції перфузійного маркера ґадолінію Gd. Інтенсивність МРТ-сигналу до ін'єкції ґадолінію прийнята за 0

An early detecting and monitoring of the tumor development and treatment efficacy are very important in chemotherapy. In this work, the capillary tissue perfusion in skeletal muscle and subcutaneous fibrosarcoma were compared to evaluate the possibility to use DCE $^{1}$H-MRI in the study of possible mechanisms of effective treatment of tumors. The Gadolinium inflow represents mostly a development of perfusion system in tissue whereas slow outflow most likely reflects a steady-state of inflow and washout of the contrast agent. The inflow was sufficiently slower in tumor tissue than that of the nearby normal muscle tissue (**Fig. 3**). The common explanation of this effect invokes an unregularly formatted blood vessels and a leaking of tumor capillaries [15]. Some contribution to the tumor vasoconstriction may be provided also an increase in number of the actively proliferated tumor cells creating pressure on the capillaries. Some tissue damages such as $CCl_4$ intoxication also lead to a decrease in inflow kinetics while outflow components did not show any significant difference [5].

In our previous studies, we showed that 5FU and cyclophosphamide significantly decreased subcutaneous RIF-1 tumor volumes developed in C3H mice [3, 4]. Li *et al.* [11] and Lemeir *et al.* [10] also reported a similar effect of 5FU therapy. At the same time points, *in vivo* MRI measurements showed an increase in both total tissue $Na^+$ NMR signal intensity and ADC in 5FU treated tumors while intracellular $Na^+$ signal intensity and glycolysis were significantly lower compared with control tumors. The correlated increases in tissue perfusion, total tissue $Na^+$ signal intensity and water ADC following chemotherapy reflect an increase in the extracellular space, vasodilatation, while the lower intracellular $Na^+$ signal intensity and glucose uptake in treated tumors compared with control tumors suggest a shift in tumor metabolism from glycolysis to oxidation and/or a decrease in cell density [4]. It was shown that 5FU therapy leads to an increase in the ATP level, ATP/$P_i$ ratio and $pH_i$ [6, 19]. An increase in the extracellular space may be an outcome of the apoptotic and/or necrotic death of tumor cells [8]. The apoptotic mechanism includes cells shrinking, blebbing of cellular membranes and developing of apoptotic bodies, while the necrotic transformation is associated with water drainage, fibrosis, cells swelling and tissue inflammation. However, both mechanisms finally lead to endocytosis and phagocytosis of tumor cells.

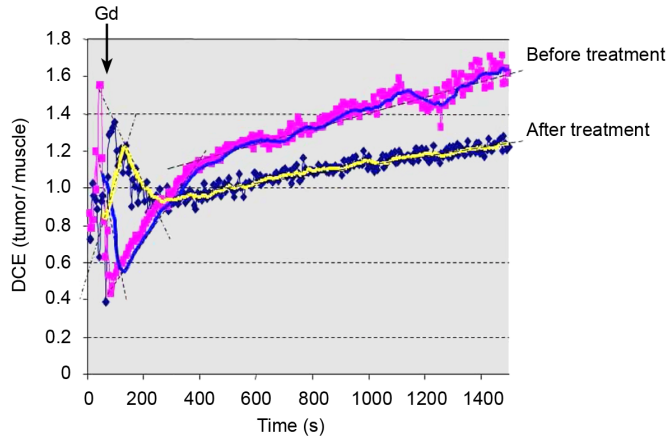


**Fig. 4.** The ratio of Diffusion Contrast Enhancement (DCE) in subcutaneous RIF-1 before and day 3 after treatment with 5-fluorouracil (150 mg/kg). Gd – Gadolinium

**Рис. 4.** Зміни співвідношення інтенсивності динамічно-контрастних $^1$H-МРТ-зображень у підшкірній радіаційно-індукованій фібросаркомі у миші лінії С3Н до (день 0) і після терапії (день 3) з 5-фторурацилом (150 мг/кг). Gd – ґадоліній

An increase in tumor blood circulation create better oxygen supply and a higher energetic status of leaving tumor cells [7, 11, 14, 18]. Post-therapeutic re-oxygenation may occur due to a number of reasons such as a decrease in distances between capillaries and their occlusion, as well as an increase in total vascularization of the tumor [17]. Therefore, an increase in both a diffusion, measured by ADC, and a perfusion, measured by DCE $^1$H-MRI, may be a promising tool to estimate early therapeutic effects prior to changes in tumor volume [9, 13].

## CONCLUSIONS

Method of dynamic contrast enhanced $^1$H-MRI in combination with other NMR methods, positron emission tomography, histology, etc. should prove useful in the assessment of neoplastic transformations of tumor capillaries and efficacy of chemotherapy.

## COMPLIANCE WITH ETHICAL STANDARDS

**Conflict of Interest:** The authors declare that the research was conducted in the absence of any commercial or financial relationships that could be construed as a potential conflict of interest.

**Human Rights:** This article does not contain any studies with human subjects performed by the any of the authors.

**Animal studies:** All institutional, national and institutional guidelines for the care and use of laboratory animals were followed.


1. *Airley R.* **Cancer Chemotherapy: Basic Science to the Clinic**. Chichester: Wiley–Blackwell, 2009. 342 p.
   Google Scholar
2. *Babsky A.M.* **Functional State of Cells and Level of $Na^+$ Under Hypoxia and Cancerogenesis**. Lviv: Ivan Franko LNU Publications, 2018. 180 p. (In Ukrainan)
3. *Babsky A., Hekmatyar S.K., Zhang H., Solomon J.S., Bansal N.* Application of $^{23}$Na MRI to monitor chemotherapeutic response in RIF-1 tumors. **Neoplasia**, 2005; 7: 658–666.
   Crossref • PubMed • Google Scholar
4. *Babsky A. M., Zhang H., Hekmatyar S. K., Hutchins G.D., Bansal N.* Monitoring chemotherapeutic response in RIF-1 tumors by single-quantum and triple-quantum-filtered $^{23}$Na MRI, $^{1}$H diffusion-weighted MRI and PET imaging. **Magnetic Resonance Imaging,** 2007; 25(7): 1015–1023.
   Crossref • PubMed • Google Scholar
5. *Babsky A., George B., Bansal N.* Assessment of hepatic perfusion and diffusion in $CCl_4$ treated rat liver using magnetic resonance imaging. **Visnyk Lviv University. Series Biology**, 2013; 61: 3–10.
   Google Scholar
6. *Bhujwalla Z.M., McCoy C.L., Glickson J.D., Gillies R.J., Stubbs M.* Estimations of intra- and extracellular volume and pH by $^{31}$P magnetic resonance spectroscopy: effect of therapy on RIF-1 tumours. **Br J Cancer**, 1998; 78(5): 606–611.
   Crossref • PubMed • Google Scholar
7. *Bhujwalla Z. M., Artemov D., Glockner J.* Tumor angiogenesis, vascularization, and contrast-enhanced magnetic resonance imaging. **Topics in Magnetic Resonance Imaging,** 1999; 10(2): 92–103.
   Crossref • PubMed • Google Scholar
8. *Braunschweiger P.G.* Effect of cyclophosphamide on the pathophysiology of RIF-1 solid tumors. **Cancer Res**, 1988; 48(15): 4206–4210.
   Google Scholar
9. *Kanematsu M., Goshima S., Watanabe H., Kondo H., Kawada H., Noda Y. Moriyama N.* Diffusion/perfusion MR imaging of the liver: practice, challenges, and future. **Magnetic Resonance in Medical Sciences,** 2012; 11: 151–161.
   Crossref • PubMed • Google Scholar
10. *Lemaire L., Howe F.A., Rodrigues L.M., Griffiths J.R.* Assessment of induced rat mammary tumour response to chemotherapy using the apparent diffusion coefficient of tissue water as determined by diffusion-weighted $^{1}$H-NMR spectroscopy *in vivo*. **MAGMA,** 1999; 8(1): 20–26.
    Crossref • PubMed • Google Scholar
11. *Li S.-J., Wehrle J. P., Glickson G., Kumar N., Braunschweiger P.G.* Tumor bioenergetics and blood flow in RIF-1 murine tumors treated with 5-fluorouracil. **Magnetic Resonance in Medicine**, 1991; 22(1): 47–56.
    Crossref • PubMed • Google Scholar
12. *Liu Y., Wang S., Zhao X., Feng Y., Bormans G., Swinnen J., Oyen R., Huang G., Ni Y., Li Y.* Predicting clinical efficacy of vascular disrupting agents in rodent models of primary and

secondary liver cancers: an overview with imaging-histopathology correlation. **Diagnostics** (Basel), 2020; 10(2). pii: E78.
Crossref • PubMed • Google Scholar

13. *Materne R., Smith A. M., Peeters F., Dehoux J.P., Keyeux A., Horsmans Y., Van Beers B.E.* Assessment of hepatic perfusion parameters with dynamic MRI. **Magnetic Resonance in Medicine,** 2002; 47: 135–142.
Crossref • PubMed • Google Scholar
14. *McSheehy P.M., Leach M.O., Judson I.R., Griffiths J.R.* Metabolites of 2′-fluoro-2′-deoxy-D-glucose detected by 19F magnetic resonance spectroscopy *in vivo* predict response of murine RIF-1 tumors to 5-fluorouracil. **Cancer Res**, 2000; 60(8): 2122–2127.
Google Scholar
15. *Nishida N., Yano H., Nishida T., Kamura T., Kojiro M.* Angiogenesis in cancer. **Vascular. Health Risk Manag.,** 2006; 2(3): 213–219.
Crossref • PubMed • Google Scholar
16. *Park H.S., Han J.K., Lee J.M., Kim Y.I., Woo S., Yoon J.H., Choi J.Y., Choi B.I.* Dynamic Contrast-Enhanced MRI Using a Macromolecular MR Contrast Agent (P792): Evaluation of Antivascular Drug Effect in a Rabbit VX2 Liver Tumor Model. **Korean J Radiol,** 2015; 16(5): 1029–1037.
Crossref • PubMed • Google Scholar
17. *Poptani H., Bansal N., Graham R.A., Mancuso A., Nelson D.S., Glickson J.D.* Detecting early response to cyclophosphamide treatment of RIF-1 tumors using selective multiple quantum spectroscopy (SelMQC) and dynamic contrast enhanced imaging. **NMR Biomed.,** 2003; 16(2): 102–111.
Crossref • PubMed • Google Scholar
18. *Poptani H., Bansal N., Jenkins W.T., Blessington D., Mancuso A., Nelson D.S., Feldman M., Delikatny E.J., Chance B., Glickson J.D.* Cyclophosphamide treatment modifies tumor oxygenation and glycolytic rates of RIF-1 tumors: $^{13}$C magnetic resonance spectroscopy, Eppendorf electrode, and redox scanning. **Cancer Res**, 2003; 63(24): 8813–8820.
Google Scholar
19. *Sijens P.E., Baldwin N.J., Ng T.C.* Multinuclear MR investigation of the metabolic response of the murine RIF-1 tumor to 5-fluorouracil chemotherapy. **Magnetic Resonance in Medicine,** 1991; 19(2): 373–385.
Crossref • PubMed • Google Scholar
20. *Sun X., Wang H., Chen F., De Keyzer F., Yu J., Jiange Y., Feng Y., Li J., Marchal G., Ni Y.* Diffusion-weighted MRI of hepatic tumor in rats: Comparison between *in vivo* and postmortem imaging acquisitions. **Journal of Magnetic Resonance Imaging**, 2009; 29: 621–628.
Crossref • PubMed • Google Scholar
21. *Sun Y., Hua R.* Ocular surface squamous neoplasia: angiographic characteristics and response to subconjunctival/perilesional 5-fluorouracil injections. **Drug Des Devel Ther**, 2019; 13: 1323–1334.
Crossref • PubMed • Google Scholar
22. *Taouli B.* (ed.). **Extra-Cranial Applications of Diffusion-Weighted MRI**. Cambridge, UK: University Press, 2011. 215 p.
Google Scholar
23. *Thoeny H. C., De Keyzer F., Chen F., Landuyt W., Verbeken E.K., Bosmans H., Hermans R., van Oosterom A., Marchal G., Landuyt W.* Diffusion-weighted magnetic resonance imaging allows noninvasive *in vivo* monitoring of the effects of combretastatin a-4 phosphate after repeated administration. **Neoplasia**, 2005; 7: 779–787.
Crossref • PubMed • Google Scholar
24. *Yankeelov T. E., Arlinghaus L. R., Li X., Gore J.C.* The role of magnetic resonance imaging biomarkers in clinical trials of treatment response in cancer. **Semin Oncol,** 2011; 38(1): 16–25.
Crossref • PubMed • Google Scholar

# ДИНАМІЧНО-КОНТРАСТНА $^{1}$H-МАГНІТНО-РЕЗОНАНСНА ТОМОГРАФІЯ ЗА ОЦІНЮВАННЯ ПЕРФУЗІЇ У СКЕЛЕТНИХ М'ЯЗАХ І ФІБРОСАРКОМІ

***А. Бабський*[1]*, *Н. Банзал*[2]**

[1] *Львівський національний університет імені Івана Франка*
*вул. Грушевського, 4, Львів 79005, Україна*

[2] *Індіанський університет, Індіанаполіс, IN 46202, США*

**Кореспондуючий автор: e-mail: andriy.babsky@lnu.edu.ua*

**Вступ.** Виявлення неоплазматичного переродження тканини і прогнозування терапевтичного ефекту є надзвичайно важливими за ефективного лікування ракових пухлин. $^{1}$H-магнітно-резонансна томографія (МРТ) є інформативним сучасним методом, який надає ексклюзивну інформацію стосовно структурних, клітинних, апоптичних і некротичних змін у пухлинній тканині. Цей метод зараз широко використовують для виявлення та моніторингу ефективності лікування. Зміни параметрів тканинної перфузії супроводжують неоплазматичне переродження тканин.

**Методи.** Метод динамічно-контрастної $^{1}$H-нмагнітно-резонансної томографії (МРТ) з перфузійним маркером (трейсером) ґадолінієм (20 мМ) був використаний для оцінки параметрів тканинної перфузії в нормальних скелетних м'язах і у підшкірній радіаційно-індукованій фібросаркомі, прищепленій на задній лапці миші лінії C3H/HeN. Терапію фібросаркоми провадили за допомогою разової ін'єкції антиметаболітного препарату 5-фторурацилу (150 мг/кг). МРТ експерименти були проведені до лікування і на третій день після ін'єкції препарату.

**Результати.** За допомогою методу динамічно-контрастної $^{1}$H-нМРТ було встановлено набагато повільнішу швидкість перфузії у підшкірній раковій тканині порівняно зі скелетними м'язами. 5-фторурацил спричиняв достовірне зниження об'єму підшкірної пухлини вже на другий і третій день після лікування. Методом ДК $^{1}$H-МРТ було встановлено, що у лікованій пухлині швидкість перфузії є суттєво збільшеною внаслідок зростання, ймовірно, об'єму позаклітинного середовища та вазодилятації пухлинних капілярів і загалом покращеної васкуляризації пухлини. Зростання швидкості перфузії корелює із нашими попередніми та літературними даними про зростання швидкості дифузії (оцінювали за показником дифузії води ADC) та рівня загального тканинного $Na^{+}$ (оцінювали за інтенсивністю сигналу $^{23}$Na-МРТ) після ефективного лікування фібросаркоми 5-фторурацилом. З іншого боку, зниження внутрішньоклітинного рівня $Na^{+}$ та зменшення поглинання глюкози після цієї терапії свідчить про зменшення кількості клітин у пухлині та про зсув пухлинного метаболізму від гліколізу до окиснення.

**Висновки.** Метод динамічно-контрастної $^{1}$H-МРТ разом з іншими методами ядерно-магнітного резонансу, позитронно-емісійної томографії, гістології та ін. може бути успішно використаний для оцінки неопластичної трансформації тканини й ефективності хіміотерапії.

***Ключові слова:*** м'язи, перфузія, ґадоліній, фібросаркома, 5-фторурацил, $^{1}$H-МРТ

Received / Одержано 19 May 2020 | Accepted / Прийнято 31 August 2020 | Published / Опубліковано 30 September 2020